Development 138, 543-552 (2011) doi:10.1242/dev.053959

Wnt/PCP signaling controls intracellular position of MTOCs during gastrulation convergence and extension movements

Diane S. Sepich*, Mohsinah Usmani, Staci Pawlicki and Lila Solnica-Krezel*,†

SUMMARY

During vertebrate gastrulation, convergence and extension cell movements are coordinated with the anteroposterior and mediolateral embryonic axes. Wnt planar cell polarity (Wnt/PCP) signaling polarizes the motile behaviors of cells with respect to the anteroposterior embryonic axis. Understanding how Wnt/PCP signaling mediates convergence and extension (C&E) movements requires analysis of the mechanisms employed to alter cell morphology and behavior with respect to embryonic polarity. Here, we examine the interactions between the microtubule cytoskeleton and Wnt/PCP signaling during zebrafish gastrulation. First, we assessed the location of the centrosome/microtubule organizing center (MTOC) relative to the cell nucleus and the body axes, as a marker of cell polarity. The intracellular position of MTOCs was polarized, perpendicular to the plane of the germ layers, independently of Wnt/PCP signaling. In addition, this position became biased posteriorly and medially within the plane of the germ layers at the transition from mid- to late gastrulation and from slow to fast C&E movements. This depends on intact Wnt/PCP signaling through Knypek (Glypican4/6) and Dishevelled components. Second, we tested whether microtubules are required for planar cell polarization. Once the planar cell polarity is established, microtubules are not required for accumulation of Prickle at the anterior cell edge. However, microtubules are needed for cell-cell contacts and initiation of its anterior localization. Reciprocal interactions occur between Wnt/PCP signaling and microtubule cytoskeleton during C&E gastrulation movements. Wnt/PCP signaling influences the polarity of the microtubule cytoskeleton and, conversely, microtubules are required for the asymmetric distribution of Wnt/PCP pathway components.

KEY WORDS: Centrosome, Prickle, Microtubule, Zebrafish, Cell polarity, Migration, Intercalation

INTRODUCTION

Cell movements are essential in the embryo to shape the axial body plan and in the adult for homeostasis and wound healing. During vertebrate gastrulation, convergence and extension (C&E) movements narrow and elongate the germ layers to form the anteroposteriorly (AP) elongated body axis that is common to vertebrate embryos (Keller, 2002; Solnica-Krezel, 2005). This morphogenetic process involves multiple cell behaviors that change according to stage and location (Roszko et al., 2009).

Non-canonical Wnt/planar cell polarity (Wnt/PCP) signaling regulates C&E in chordates from ascidians through mammals by polarizing the morphology and behavior of cells (Jiang et al., 2005; Solnica-Krezel, 2005). Wnt/PCP signaling organizes sheets of cells to exhibit a consistent polarity perpendicular to the axis of the apical-basal polarity (Axelrod and McNeill, 2002; Eaton, 2003; Fanto and McNeill, 2004). In *Drosophila*, where planar cell polarity was discovered, PCP signaling is required to coordinate the orientation of epithelial structures in the cuticle, wing, and eye (Gubb and Garcia-Bellido, 1982; Adler, 2002). Downstream of an asymmetry cue (Strutt and Strutt, 2009), transmembrane proteins Frizzled (Fz) and Vangogh (Vang) are required in adjacent cells to initiate planar polarization. Other components of the Wnt/PCP pathway, Dishevelled (Dvl) and Prickle (Pk), amplify the difference leading to visible asymmetry in protein distribution; Fz and Dvl are found at the distal side of the cell where a hair forms, while antagonistic factors Vang and Pk are enriched at the opposite cell membrane (Usui et al., 1999; Axelrod, 2001; Feiguin et al., 2001; Shimada et al., 2001; Strutt, 2001; Tree et al., 2002; Bastock et al., 2003; Narayan et al., 2004; Simons and Mlodzik, 2008).

Wnt/PCP signaling most commonly controls polarity in epithelia, where cells tend to maintain close cell-to-cell contact. However, during vertebrate gastrulation, Wnt/PCP also influences polarity in mesenchymal cells that form transient cell contacts (Jessen et al., 2002; Marlow et al., 2002). Wnt/PCP signaling promotes polarized cell migration and rearrangements and coordinates this polarity with embryonic axes. These polarized movement behaviors include directed migration, mediolateral intercalation (Wallingford et al., 2000; Jessen et al., 2002) and polarized radial cell intercalation (Yin et al., 2008). Furthermore, oriented cell divisions also require Wnt/PCP signaling (Gong et al., 2004; Ciruna et al., 2006). Under the influence of Wnt/PCP signaling, cells elongate and align mediolaterally, and thus perpendicular to the AP gastrula axis. In addition, the direction and stability of protrusions, and movement direction of cells, are mediolaterally biased (Wallingford et al., 2000; Topczewski et al., 2001; Jessen et al., 2002; Montero et al., 2005). Mechanistically, Wnt/PCP signaling influences dynamic cohesion of anterior mesoderm cells (Montero et al., 2005), endocytosis of E-cadherin molecules (Ulrich et al., 2005), and the distribution of Fibronectin (Goto et al., 2005; Yin and Solnica-Krezel, 2007).

Such striking polarization of cell behaviors suggests Wnt/PCP influences the microtubule (MT) cytoskeleton. Evidence implicates Wnt/PCP signaling in orienting the basal body in cochlea, floor plate of the neural tube, and epidermis, suggesting an interaction

Department of Biological Sciences, Vanderbilt University, Nashville, TN 37212, USA.

*Present address: Department of Developmental Biology, Washington University School of Medicine, St Louis, MO 63110, USA
†Author for correspondence (sepichd@wustl.edu)

Accepted 24 November 2010

with the centrosome or microtubule organizing center (MTOC) (Jones and Chen, 2008; Park et al., 2008; Borovina et al., 2010). As the MTOC organizes the MT cytoskeleton, Golgi complex, cilium and the proteasome, its position polarizes many cellular functions (Badano et al., 2005). Here, we begin to examine the influences of Wnt/PCP on the MT cytoskeleton during gastrulation by testing whether Wnt/PCP signaling can control the position of the MTOC.

The asymmetric accumulation of PCP components, so obvious in *Drosophila* epithelia (Simons and Mlodzik, 2008), has been difficult to document in migrating cells of vertebrate gastrulae. However, recent studies showed anterior membrane localization of exogenous *Drosophila* Prickle-GFP in the neural plate and mesoderm (Ciruna et al., 2006; Yin et al., 2008), and posterior accumulation of *Xenopus* Dishevelled-GFP in mesoderm during zebrafish gastrulation (Yin et al., 2008). The molecular mechanisms that establish the asymmetric distribution of the Wnt/PCP pathway components remain incompletely understood (Strutt and Strutt, 2007). However, in *Drosophila* epithelia, intact MTs are needed for proper Fz localization. Furthermore, Fz-GFP protein travels along MTs toward the distal cell edge before its asymmetric accumulation is apparent (Shimada et al., 2006).

Here we have investigated interactions between Wnt/PCP signaling and the MT cytoskeleton in zebrafish gastrulation cell movements that differ in their dependence on Wnt/PCP signaling (Fig. 1A,B). First, we find that MTOCs have a biased location along the superficial-deep axis of the embryonic tissues, suggesting an emerging apical-basal polarity. Second, we find that MTOCs occupy a polarized position within the plane of the ectoderm and mesoderm, becoming biased to the posterior and dorsal/medial side of the cell between mid and late gastrulation. We find that interfering with the Wnt/PCP signaling components Knypek/Glypican4/6 (Kny/Gpc4) and Dvl randomizes MTOC position in the planes of the ectoderm and mesoderm.

Third, we asked whether the establishment and maintenance of mediolateral and AP cell polarity mediated by Wnt/PCP signaling requires an intact MT cytoskeleton. We find that disruption of the MT cytoskeleton at midgastrulation, before the onset of Wnt/PCP signaling, blocks clustering of Prickle-GFP at the anterior cell membranes. By contrast, disruption of the MT cytoskeleton when cells are mediolaterally elongated did not eliminate Pk-GFP puncta from the membrane, or block their anterior location. Hence, MTs are needed for the establishment, but not for the maintenance, of the anterior Pk localization.

Together, our studies of MTOC intracellular position show a nascent polarity aligned with the future apicobasal polarity and planar cell polarity in cells undergoing C&E during gastrulation. Moreover, we reveal complex mutual interactions between components of Wnt/PCP signaling and the MT cytoskeleton; some positively acting components (Dvl and Kny/Gpc4) are required for polarized MTOC position. In turn, an intact MT cytoskeleton is not necessary for the maintenance of Prickle, a Wnt/PCP protein, at the anterior cell membrane during C&E, but is needed for the establishment of this polarity.

MATERIALS AND METHODS

Zebrafish maintenance, embryo generation, and staging

AB* wild-type zebrafish and fish carrying mutations in *knypek*^{fr6} (Topczewski et al., 2001) were maintained as described (Solnica-Krezel et al., 1994). Naturally spawned embryos were raised at 26-32°C, and staged according to their morphology (Kimmel et al., 1995). Transgenic Tg(XlEef1a1:dclk2DeltaK-GFP)io007 fish (a gift from Marina Mione, Milan, Italy) were used to test nocodazole effectiveness. We use descriptive terms to denote gastrulation stages: 'start of gastrulation' refers to shield stage (6 hpf), 'midgastrulation' refers to 75 to 85% epiboly (8-8.7 hpf) and 'late gastrulation' refers to yolk plug closure to the one-somite stage (9.5-10.2 hpf).

Constructs, stains and antibodies

RNA was synthesized with (mMESSAGE mMACHINE; Ambion) and injected into one- or two-cell embryos at the following doses: *Xdd1* (400 pg), membrane-localized (i.e. CAAX/Ras membrane-localization domain) *RFP* or *Cherry* (200-400 pg) (a gift from Fang Lin, University of Iowa, IA, USA), *Xenopus EGFP centrin* (5-40 pg) (a gift from Adrian Salic and Kristin Kwan, Harvard Medical School, MA, USA). Embryos were fixed overnight in 4% paraformaldehyde in PBS, permeabilized in 0.5% Triton in PBS 30-60 minutes at room temperature and labeled with anti-acetylated tubulin MAb (1/800 Sigma T6557) or anti γ-tubulin (1/250 Sigma T6793).

Pk and nocodazole experiments

Embryos were injected with RNAs coding for RFP-CAAX (Jason Jessen, Vanderbilt University Medical Center, TN, USA) at the one-cell stage and for *Drosophila* Pk-GFP (Jenny et al., 2003) with or without Histone2A-RFP at the 8- to 32-cell stage and allowed to develop until mid or late gastrulation. Dechorionated embryos were grown for 30-120 minutes in 28 or 32°C Danieau's buffer with 0, 5 or 10 μg/ml nocodazole.

Confocal imaging and data analysis

Live embryos were mounted in 2% methylcellulose or 0.5% low-melting-point agarose (Seaplaque catalog number 50100) in 30% Danieau's buffer (Saude et al., 2000) on glass-bottomed dishes (Matek PG35G-0-10-C or Willco Wells BV-0310-35). Confocal and DIC *z*-stacks (0.5-4 μm spacing) were collected from dorsal regions with a Zeiss LSM 510 microscope using 20× or 40× oil-immersion (NA 1.3) objectives, or spinning disk confocal using a 40× oil-immersion (NA 1.3) objective mounted on a motorized Zeiss Axiovert 200 and a PerkinElmer ERS spinning-disk confocal system. The positions of the cell nucleus (visible in DIC or by diffuse Centrin labeling) and MTOC (Centrin-labeled) were marked in Object-Image (NIH image) and exported to Excel (Microsoft), where angle was calculated. Cells containing two well-separated MTOCs (greater than 7-10 μm) were not counted. Cell divisions (cells with two opposite MTOCs and furrowing of membrane) were described as 'aligned with the AP axis' if they were within 45° of the axis. Further analysis was performed using LSM-Browser (Zeiss), Image J (NIH), Object Image (Norbert Vischer), Volocity (Improvision) and Excel (Microsoft). Standard error of the mean (s.e.m.) was calculated as (standard deviation/$\sqrt{}$sample size). VectorRose (Watson's two-sample U^2 test, PAZsoftware, Pierre A. Zippi) was used for statistical analysis.

RESULTS

Dynamic centrosome localization and behavior during zebrafish gastrulation

To gauge polarity of the MT cytoskeleton in gastrula cells, we examined the location of the centrosome, labeled by injection of *Xenopus centrin-gfp* RNA. Centrin is a component of the distal side of the centriole, a structure that serves several functions in the cell, including organizing MTs during cell division and interphase, and acting as the basal body of a cilium (Dawe et al., 2007).

Antibody against γ-tubulin and fluorescently labeled *Xenopus* Centrin (eGFP-Xcentrin) fusion protein co-labeled (data not shown, DNS) small, tightly focused and usually paired spots that could be found in nearly all cells of the zebrafish gastrula; we interpret these to be centrioles (Fig. 1E). We injected synthetic RNA encoding eGFP-Xcentrin into 1- to 16-cell stage embryos. Centrosomes were often found close to the cell membrane, and were sometimes close to centrosomes in an adjacent cell (Fig. 1F,G). Furthermore, some centrioles localized to the tips of intracellular projections of the plasma membrane, which followed the centrioles as they moved (Fig. 1G, blue arrow). Time-lapse recordings showed that centrioles

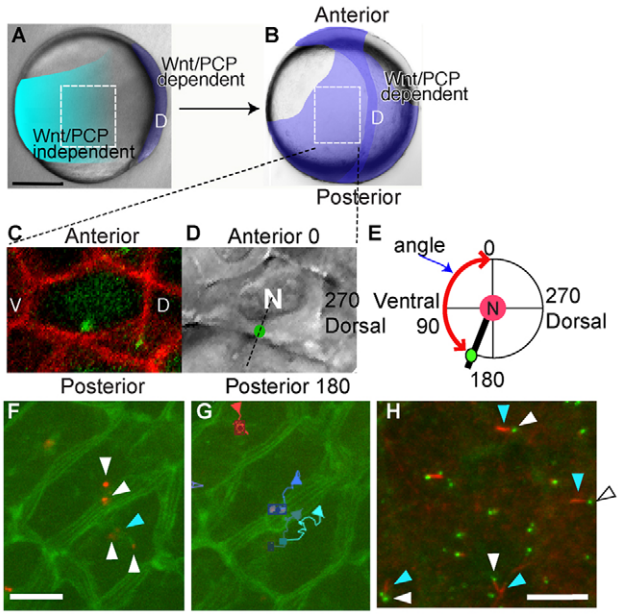

Fig. 1. Embryonic regions examined, methods for MTOC position measurement and some functions of centrin-labeled MTOCs. (**A**) In a midgastrulation embryo, Wnt/PCP signaling is required in cells of the dorsal midline (D) for convergence and extension, but not in lateral regions. The regions within the dotted white line were examined for MTOC angle. Scale bar: 200 µm. (**B**) Late gastrulation embryo. Lateral mesodermal cells flank the notochord and require Wnt/PCP signaling to migrate efficiently. (**C**) Membrane (red) and centrosome (green) labeling. Cells were oriented so that anterior of the embryo was oriented towards the top of the frame during measurement. Dorsal (D) and ventral (V) in the embryo are indicated. (**D**) Nucleus is visible in DIC optics with a green dot denoting an overlain MTOC. Dotted black line indicates orientation of MTOC relative to the nucleus. Distance between MTOC and nucleus was not measured. (**E**) Illustration of how MTOC position was measured relative to the nucleus N and the embryonic body axes. Angle measured is indicated by the red line. (**F**) Centrosomes (*Xenopus* centrin-Cherry, white arrowhead) in projected *z*-stack have a membrane connection to the cell membrane. (CAAX-EGFP, blue arrowhead). (**G**) Centrosomes move in cells. Paths followed for 10 minutes start at the square. (**H**) Short cilia (red, acetylated tubulin, white arrowhead) colocalize with some centrosomes (eGFP-Xcentrin, blue arrowheads). Scale bars: 10 µm.

moved rapidly in cells, as has been reported for cultured cells [Fig. 1G, average instantaneous speed 2.14 µm/minute, s.e.m. 0.53, average net speed 0.61 µm/minute s.e.m. 0.26, n=1 YPC embryo, 122 cells (Piel et al., 2000)].

To learn whether centrosomes serve as basal bodies during late gastrulation, we labeled centrosomes with eGFP-Xcentrin and cilia with an antibody against acetylated tubulin. Short presumptive cilia are seen on the outermost enveloping layer cells from as early as midgastrulation (80% epiboly, 8 hours post fertilization, hpf, DNS). By segmentation, some centrosomes were found abutting presumptive cilia (Fig. 1H, blue arrowhead) in neural plate and mesoderm, and in the interior of the notochord (DNS). The plasma membrane attached to centrosomes may enclose the intracellular parts of cilia, as these structures are approximately the same length (compare Fig. 1F, blue arrowhead with Fig. 1H).

Cells in an epithelial tissue can be polarized over multiple axes, for example, across the plane of an epithelial sheet (i.e. planar polarity), as well as across the thickness of the tissue (i.e. apical-basal polarity). In epithelia, centrosomes are typically located near the apical surface (Hay, 2005; Baum et al., 2008; Hong et al., 2010), whereas in migrating mesenchymal cells, centrosomes frequently assume a position between the leading edge and the nucleus. During zebrafish gastrulation, lateral ectoderm and mesoderm cells migrate towards the dorsal midline as a cohesive sheet or as individual cells, respectively (Solnica-Krezel, 2005). Near the midline, mesenchymal mesoderm cells cohere to form a cohesive body axis. We wondered whether MTOC position was polarized relative to the superficial-deep axis of the germ layers during these migrations. We labeled cell membranes and centrosomes by injection of synthetic RNA encoding membrane-localized red fluorescent protein (membrane-RFP) and green fluorescent protein *Xenopus* centrin fusion (GFP-centrin) protein, respectively. We collected *z*-stacks from the resulting mid and late gastrulae and made orthogonal reconstruction stacks of the lateral region (above the blastoderm margin, about 13 cells wide) at midgastrulation and the region immediately adjacent to the notochord (seven cells wide, at the equator) at late gastrulation (Fig. 1A,B). These images showed the position of MTOCs relative to the germ layer boundaries in both ectoderm and mesoderm (Fig. 2A-F). We observed that MTOCs were present preferentially near the superficial side of the ectodermal cells. Intriguingly, MTOCs were largely absent from the ectoderm/mesoderm boundary. Within the mesoderm, MTOCs were found toward the interior of the germ layer. Quantification of the average MTOC position relative to the germ layer thickness position in three mid- and two late wild-type gastrulae and in two *kny*$^{-/-}$ gastrulae was consistent with this visual impression from previous embryos (Fig. 2G). Based on these observations, we conclude that gastrula cells exhibit polarity along the superficial-deep axis of the germ layers, possibly representing a nascent apical-basal polarity by midgastrulation that is independent of Wnt/PCP signaling.

MTOCs acquires a biased position in cells engaged in C&E

Cells engaged in C&E also become polarized within the tissue plane, i.e. planar cell polarity (Wallingford et al., 2000; Topczewski et al., 2001; Jessen et al., 2002; Marlow et al., 2002; Myers et al., 2002). Our current and previous studies have examined cells that begin gastrulation at the lateral margin. These mesodermal cells demonstrate different migration behaviors and dependence on Wnt/PCP signaling at mid and late gastrulation. At midgastrulation, these moderately elongated and loosely packed cells (Jessen et al., 2002; Sepich et al., 2005) converge dorsally and become distributed in an anteroposteriorly elongated array of highly packed and mediolaterally elongated cells. Our observations were centered on cells at the embryonic equator; by the one-somite stage, these equatorial cells contribute to the first two somites and the anterior mesoderm. Consequently, we examined mesoderm at midgastrulation when cells are about 75° from the midline (Fig. 1A), and again at late gastrulation when cells quickly traverse a region 55-20° from the midline (Fig. 1B). At midgastrulation, the germ layers are one or two cells thick with irregularly shaped cells, consistent with lower cell density. Thickness of the germ layers remains similar at late gastrulation, as cells become densely packed; when somites form, well-organized two-cell-thick tissues appear (Fig. 2A,B and DNS).

To determine whether the MTOCs have a polarized position within the plane of the germ layer in this one cell population at mid and late gastrulation, we collected simultaneous confocal and differential interference contrast (DIC) *z*-stack images to reveal the

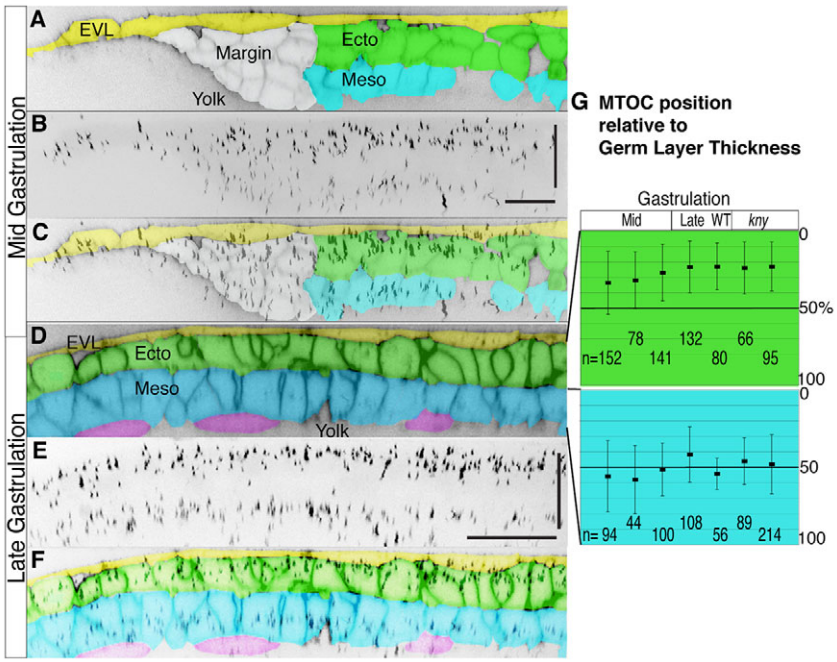

Fig. 2. MTOC has a stereotyped position perpendicular to the germ layers during gastrulation. (**A**) One slice from an orthogonally reconstructed *z*-stack showing cells in ectoderm (green), mesoderm (blue), enveloping layer (yellow) and the involuting margin (white). MTOC position was measured in the blue and green regions. (**B**) *Z* projection shows MTOC across the lateral region revealing biased location. (**C**) Merge of two above images. (**D**) One slice from an orthogonally reconstructed *z*-stack showing cells in ectoderm (green), mesoderm (blue), enveloping layer (yellow) and endoderm (purple). (**E**) *Z* projection shows all the MTOC across the seven-cell wide region beside the notochord revealing biased location. (**F**) Merge of two above images. (**G**) To determine MTOC relative to germ layer thickness, orthogonal *z*-stacks were made so that MTOC position and germ layer thickness could be measured. MTOC in the ectoderm at 0% germ layer is at the most superficial side, while 100% germ layer is at the ecoderm/mesoderm boundary. Average position relative to germ layer is plotted, with standard deviation for individual embryos, *n* is number of observations from each embryo (s.e.m. is two or three). Scale bars: 30 μm.

orientation of the nucleus-MTOC axis relative to the body axes of the embryo (Fig. 1A-E). As illustrated, we calculated the position of the MTOC relative to the nucleus and the body axes, and described this relationship as an angle relative to the anterior side of the embryo (see Fig. 1E). At midgastrulation, when lateral cells are only moderately elongated (length-to-width ratio, LWR=1.4±0.28) (Jessen et al., 2002), we found no evidence of polarization of MTOC position. MTOCs were randomly oriented with respect to the nucleus and embryonic axes (Fig. 3; Tables 1 and 2). However, we found that by late gastrulation, MTOC position became biased in both ectodermal and mesodermal cells (Fig. 3). At yolk plug closure (9.5 hpf) and tailbud (10 hpf) stages, the most common position for MTOCs was posterior of the nucleus or posterior and slightly dorsal/medial of the nucleus (Fig. 3, Table 1). This bias was not correlated with the direction of migration, which is dorsalward at this time (*n*=3 embryos, *n*=58 ectodermal cells, average direction 266° from anterior, *n*=57 mesodermal cells, average direction, 263°). By the one-somite stage (10.2 hpf), the most common position for the MTOC was posterior-dorsal or posterior-ventral of the nucleus relative to the body axes. The distributions of MTOC orientations were statistically different from a random distribution, and different from the orientation of MTOC found in cells at earlier stages of gastrulation (Tables 1, 2). Therefore, we conclude that MTOCs acquire a biased position with respect to the AP axis within cells engaged in C&E movements at late gastrulation.

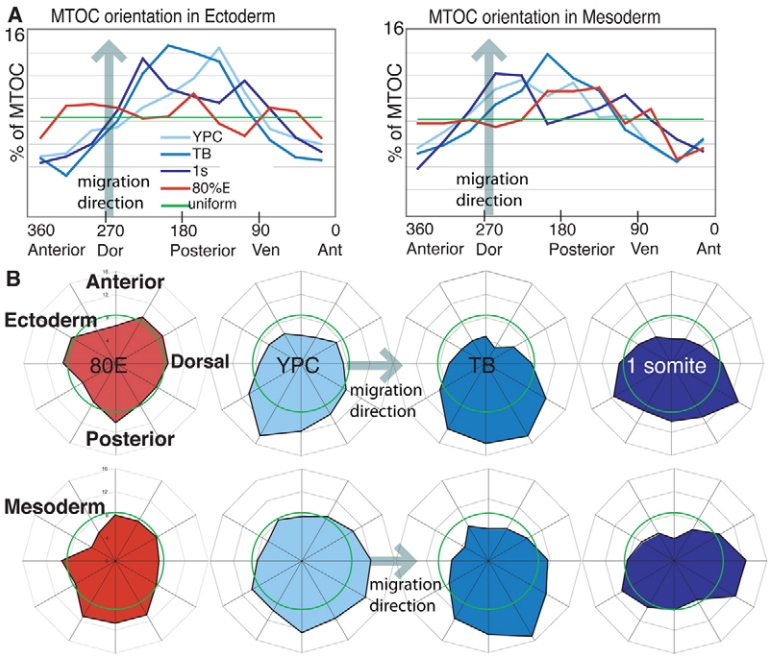

Fig. 3. MTOC position becomes biased during gastrulation. (**A**) MTOC orientation in wild-type embryos, at 80% epiboly (8 hpf), yolk plug closure (10 hpf), tailbud (10.5 hpf) and one-somite stages (11.3 hpf) in ectoderm or mesoderm. Data are graphed as percentage of centrosomes in each of twelve directions. Anterior is 0, posterior is 180, dorsal is 270 and ventral is 90. The green line indicates a uniform distribution. (**B**) The same data are presented as radar graphs. The outermost ring of the graph is set at 16% of cells. A uniform distribution of centrosomes is indicated by the green ring (8.3%).

The labeling method did not disturb the normal orientation of cell division, which appeared to be normally aligned with the AP axis. Dividing cells were counted separately and were defined as round cells or cells with an obvious cleavage furrow and two centrioles, which defined spindle orientation. In addition, cells with two centrosomes separated by more than a small distance (~5 μm) were excluded from orientation analysis, as nuclear/centrosome orientation could not be uniquely defined. Previous work has shown that more than 90% of dividing cells in ectoderm during gastrulation were aligned within 45° of the AP axis (Gong et al., 2004). Accordingly, we observed that more than 82% of dividing ectodermal and 69% of mesodermal cells aligned their division plane with the AP axis at late gastrulation (9.5-10.2 hpf, 17 embryos, *n*=101/123 and 32/46 divisions, respectively, composite 78%, *n*=133/169) and at midgastrulation (75-85% epiboly, 11 embryos, 8-8.7 hpf, 72 and 75% aligned in ectoderm and mesoderm, respectively, *n*=13/18 and 6/8 divisions; Table 3).

The biased position of MTOC depends on normal function of some Wnt/PCP components

Wnt signaling is required for reorientation of the MTOC in fibroblasts in the cell culture scratch assay (Schlessinger et al., 2007). The implicated Wnt pathway involves elements of canonical signaling (the DIX domains of Dvl and Axin, and inhibition of GSK3β) and Wnt/PCP signaling (the ligand Wnt5, which can stimulate canonical or Wnt/PCP signaling) (Mikels and Nusse, 2006; Cha et al., 2008; Mikels et al., 2009).

To test whether Wnt/PCP signaling regulates MTOC polarity in dorsally migrating cells during zebrafish gastrulation, we manipulated Wnt/PCP signaling by two means and analyzed the consequences on the intracellular position of MTOCs during late gastrulation. We found that when Wnt/PCP signaling was impaired, the distribution of MTOC positions differed from that found in wild-type gastrulae and often was indistinguishable from the random distribution. First, we altered the function of Dvl, a pathway component common to both Wnt/β-catenin and Wnt/PCP signaling, by overexpressing synthetic RNA coding for the dominant-negative Xdd1 mutant protein. According to earlier studies, overexpression of Xdd1 in the dose range used here inhibits the Wnt/PCP pathway and C&E without affecting patterning and thus canonical Wnt signaling. Accordingly, embryos overexpressing Xdd1 exhibited shortened bodies, synopthalmia or cyclopia, and reduced elongation and alignment of mesodermal cells (Tada and Smith, 2000; Wallingford et al., 2000; Jessen et al., 2002) (see Fig. S1 in the supplementary material; 400 pg Xdd1). Notably, MTOCs were positioned randomly in ectoderm and randomly or anteriorly in mesoderm in gastrula cells at late gastrulation (YPC and TB stages, Fig. 4, Tables 1 and 2). Moreover, dividing cells were less well aligned with the AP axis compared with wild-type embryos (59% of 46 dividing cells in five Xdd1-injected versus 78% aligned in 17 wild-type embryos, Table 3), but not as disturbed in this experimental setting as previously reported, suggesting Wnt/PCP signaling was reduced but not absent (Gong et al., 2004).

Second, we examined MTOC orientation in embryos homozygous for the null *fr6* allele of *knypek* (*kny*^{fr6}/*gpc4*), a positively acting component of the Wnt/PCP pathway (Topczewski et al., 2001). In these zygotic mutants, we found that MTOCs were positioned randomly in ectoderm and randomly or anteriorly in mesoderm at late gastrulation (Fig. 4, Tables 1, 2). We observed disturbed cell division orientation in *kny* embryos compared with wild-type siblings (64% aligned, 121 dividing cells in eight embryos, Table 3), consistent with impaired Wnt/PCP activity.

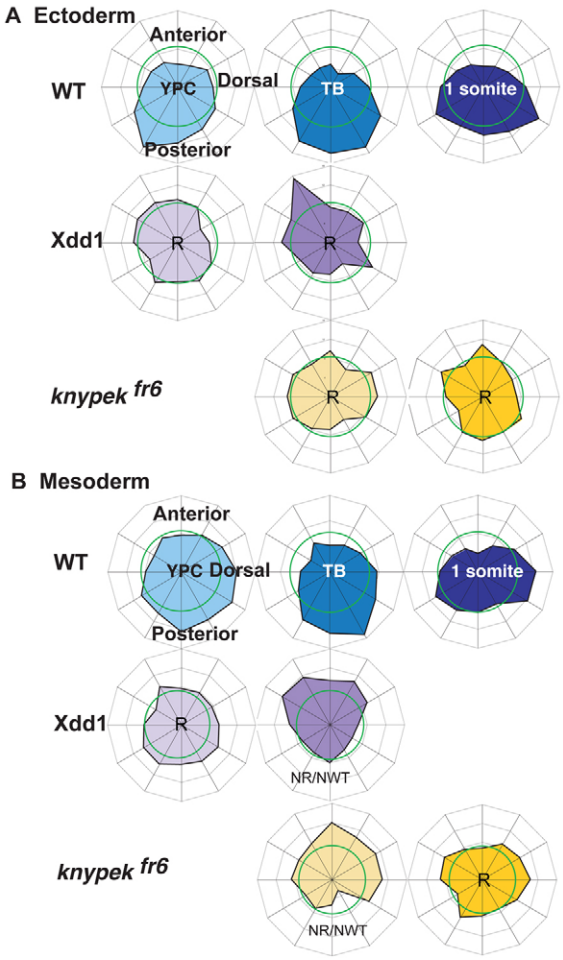

Fig. 4. Biased MTOC position depends on some components of Wnt/PCP signaling. (**A**) MTOC distributions in ectoderm in wild type and in embryos with reduced Wnt/PCP signaling, Xdd1-injected or *knypek* mutants, and (**B**) MTOC distributions in mesoderm in wild type and embryos lacking Wnt planar cell polarity signaling. Wnt/PCP signaling, Xdd1-injected or *knypek* mutants. A uniform distribution of centrosomes is indicated by the green ring (at 8.3%). The outermost ring of the graph is set at 16% of cells. NR/NWT denotes distributions that are statistically neither like random nor like wild type. R denotes random distributions.

Are MTOC distributions in the Wnt/PCP gastrulae different from wild-type distributions and different from random ones? Relatively few observations came from individual embryos; distributions only emerged when data was combined from several embryos. Each Wnt/PCP-depleted scenario was compared with a random distribution and to the sample collected from stage matched control wild-type embryos, using the Watson's U^2 test of circular data and a significance limit of 1% (Table 1). We found that the distributions of MTOCs in Wnt/PCP-depleted embryos differed at every stage from those in control gastrulae. Moreover, distributions of MTOCs in the ectoderm of Wnt/PCP-depleted embryos were not different by statistical analysis from data expected for a random distribution. The results for mesoderm were mixed. Data from *kny* at 1 somite stage and from Xdd1 at YPC stage were indistinguishable from a random distribution. Statistical analysis indicated data from tailbud stages barely exceeded the critical value of U^2, indicating difference from a random population. These distributions appeared to have an anterior bias. Consequently, we observe that distribution

Table 1. Are mutant distributions different from wild-type distributions and different from random distributions?

		Ectoderm				Mesoderm			
		80E	YPC	TB	1s	80E	YPC	TB	1s
Wild type	versus random	0.067	1.53	5.14	1.46	0.166	1.22	1.66	0.763
knypek	versus random			0.053	0.055			0.28	0.09
	versus same age wild type			1.50	0.84			1.19	0.44
Xdd1	versus random		0.104	0.11			0.064	0.34	
	versus same age wild type		0.802	1.13			0.511	1.68	

Statistical significance, at 1% level, was determined using Watson's U^2 test of circular data. The mutant distribution was compared with a random distribution and to the sample collected from same age wild-type embryos. The null hypothesis is that the samples are drawn from the same parent population. If U^2 is greater than or equal to 0.268, the null hypothesis is rejected; the mutant distribution is from different parent populations than the compared wild type or random distribution. Red are random, blue are not random, green are different from wild type. Wnt/PCP-depleted distributions are all different from wild type ones. In all but two cases, Wnt/PCP-depleted distributions are statistically indistinguishable from a random distribution.

of MTOCs in Wnt/PCP-depleted embryos is altered from that observed in control gastrulae, and this probably represents randomization or an anterior bias of MTOC position.

In summary, reducing the function of two positively acting Wnt/PCP signaling components, Dvl and Kny/Gpc4, resulted in randomization of a polarized trait, the intracellular position of the MTOC during late gastrulation. Based on these observations, we propose that Wnt/PCP signaling can bias the intracellular localization of MTOCs.

MTs are required for the establishment of AP cell polarization during gastrulation

PCP signaling in *Drosophila* wing primordia results in the asymmetric localization of PCP components across each cell. Fz and Dvl proteins accumulate distally, whereas Vang and Pk localize proximally (Strutt and Strutt, 2007; Axelrod, 2009; Amonlirdviman et al., 2005; Wu and Mlodzik, 2008). Frizzled protein is proposed to initially arrive at the distal side through an asymmetric transport of vesicles along MTs aligned with the proximo-distal wing axis (Shimada et al., 2006). Accumulation of the Wnt/PCP component, Pk, at the anterior cell edges has also been observed during C&E in ascidians and zebrafish gastrulae (Jiang et al., 2005; Ciruna et al., 2006; Yin et al., 2008). This anterior localization is lost or reduced in embryos deficient in Wnt/PCP components Dvl, Kny/Gpc4 and Tri/Vangl2 (Ciruna et al., 2006; Yin et al., 2008). Moreover, in *tri/kny* compound mutants, Pk-GFP remains mostly unclustered in the cytosol (Yin et al., 2008). To begin to address the cellular mechanism by which Wnt/PCP components become asymmetrically localized during C&E, we asked whether an intact MT cytoskeleton was needed for the establishment and/or maintenance of Pk localization at the anterior cell membrane in dorsal mesoderm and ectoderm. To find a treatment capable of depolymerizing MTs, we exposed dechorionated embryos carrying a transgene for a GFP-tagged microtubule-binding protein (TgXlEef1a1:dclk2DeltaK-GFP) to nocodazole (5 or 10 μg/ml) starting at midgastrulation or at YPC, continuing 1 or 2 hours. We found that 5 μg/ml nocodazole efficiently depolymerized MTs in mid or late gastrulae, as previously reported (Strahle and Jesuthasan, 1993; Solnica-Krezel and Driever, 1994). Fine MTs were completely absent. Infrequent large bundles of MTs were seen in the enveloping layer cells at all stages and in deep cells at late gastrulation. With longer exposure, even these few MT bundles disappeared, and diffuse fluorescence shifted into the nuclei (see Fig. S2 in the supplementary material).

To determine whether MTs were needed for the initial clustering of Pk at the anterior membrane, Pk-expressing dechorionated embryos were exposed to nocodazole from midgastrulation (8 hpf) until their siblings completed epiboly (about 2 hours, 10.2 hpf). Images were collected by confocal microscopy at the dorsal midline of the embryo to visualize Pk protein accumulation in the notochord, presomitic mesoderm and neural ectoderm. Embryos treated at 80% epiboly failed to close the blastopore; C&E continued as evidenced by the formation of a thicker axis and a small head bulge. Essentially all deep cells became rounded (five embryos, 201 cells, LWR 1.22±0.22) and appeared to lose cell-cell contacts (Fig. 4C and DNS). GFP-Pk clusters were absent. Based on these observations, we conclude that cell-cell contact and subsequent clustering of Pk require intact MTs.

To determine whether MTs were needed to maintain anterior Pk localization, we treated embryos with nocodazole from YPC to the one-somite stage (9.5-10.3 hpf). C&E was partly delayed (DNS) and the embryos were sharply elongated, similar to weakly dorsalized mutants (Mullins et al., 1996). This morphological defect demonstrates a requirement for MTs even after blastopore closure. However, cells maintained mostly elongated morphology (LWR in wild-type notochord cells 2.01±0.59, 226 cells, five embryos versus nocodazole-treated 1.97±0.59, 179 cells, seven embryos). Regarding Pk-GFP distribution, the cells were classified as previously described (Yin et al., 2008): spots limited to the anterior membrane, spots or uniform labeling not limited to the anterior membrane or cytosolic labeling. Surprisingly, the anterior enrichment of Pk-GFP puncta was maintained or decreased slightly (Fig. 5D) nocodazole-treated (n=7) compared with control (n=7) embryos. These results support the notion that intact MTs are required for initial clustering and anterior localization of Pk, either directly or by making membranes competent to accumulate Pk,

Table 2. Number of observations of MTOC position

		Ectoderm			Mesoderm		
		YPC	TB	1s	YPC	TB	1s
Wild type	Cells	744	1132	430	816	779	166
	Embryos	7	10	4	9	9	3
zygotic *knypek*$^{fr6-/-}$	Cells	ND	280	485	ND	476	389
	Embryos	ND	2	5	ND	4	3
Xdd1 (400pg)	Cells	568	137	ND	735	325	ND
	Embryos	5	2	ND	5	3	ND

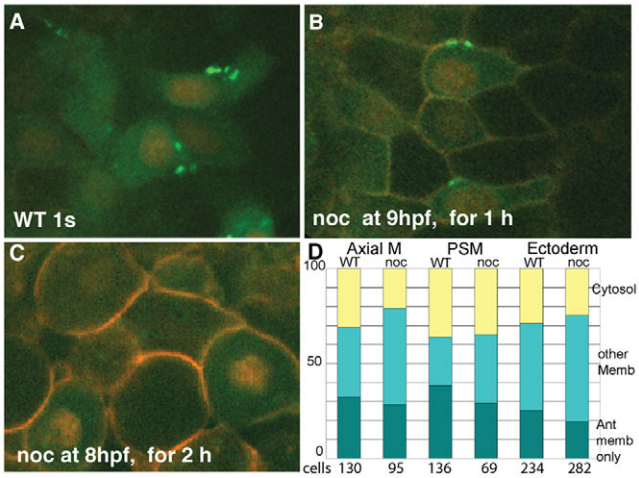

Fig. 5. Intact microtubules are not required for Pk maintenance at anterior cell membrane, but are need for establishment of anterior localization. In all panels, embryos are one-somite stage and anterior is upwards; cells are presumptive mesoderm (at least one cell layer away from the enveloping layer cells or clearly below ectoderm/mesoderm boundary). Cells are labeled with Histone2B-RFP, Membrane-RFP and Pk-GFP. (**A**) Wild-type embryo grown without nocodazole, (**B**) grown in 10 µg/ml nocodazole for 1 hour, starting at late gastrulation or (**C**) grown in 10 µg/ml nocodazole for 2 hours, starting at midgastrulation. (**D**) The location of Pk-GFP labeling was noted for axial mesoderm, presomitic mesoderm (PSM) and ectoderm in wild-type and 1 hour nocodazole-treated embryos (*n*=7, each condition). Cellular localization is largely stable to 1 hour treatment.

perhaps through cell-cell adhesion or anterior membrane identity. Once Pk accumulation at the cell anterior is established, MTs are not needed for its maintenance. We propose that MTs are required to establish, but not to maintain, the anterior localization of Pk during C&E. Together, our observations reveal reciprocal functional interactions between MTs and Wnt/PCP signaling in the process of cell polarization during vertebrate gastrulation.

DISCUSSION

Centrosome position reveals two axes of cell polarity during gastrulation

Here, we have analyzed the intracellular position of the MTOC during zebrafish gastrulation. MTOC is in vigorous, often back and forth, motion in gastrula cells (Fig. 1G), similar to observations from cultured cells (Piel et al., 2000). Despite this dynamic nature, analyses of populations of MTOCs showed that they have preferred locations within the cell at distinct stages of gastrulation. Our observations reveal that intracellular positions of MTOC are polarized along two axes. First, by midgastrulation, MTOCs are polarized along a superficial-deep axis through the ectoderm and mesoderm. Second, MTOCs become polarized within the planes of the ectoderm and mesoderm; this planar polarization of MTOCs emerges between mid and late gastrulation.

By midgastrulation, the germ layers are well separated into a superficial ectodermal sheet and deeper mesendoderm layer (Warga and Kimmel, 1990; Concha and Adams, 1998). At this stage, MTOCs display a biased position along the superficial-deep axis of the ectoderm (Fig. 2), but no obvious polarity with respect to the direction of cell migration or body axes (Fig. 3). In the ectoderm, MTOCs were found enriched near the surface of the embryo, suggesting that ectodermal cells orient their presumptive apical surfaces towards the outside and their basal ones towards the inside of the embryo. By contrast, in the mesoderm, MTOCs were found toward the interior of the germ layer (Fig. 2). We speculate that this asymmetric distribution of MTOCs in the germ layers at midgastrulation reflects an early step toward a well-organized apical-basacellular axis.

Several observations suggest that germ layers gradually acquire polarity along the apical-basal axes during zebrafish gastrulation. Epithelia typically form a cellular sheet bounded basally by extracellular matrix (ECM), with basally positioned nuclei and apically located centrosomes or cilia and tight junctions (Thiery, 2002; Barrios et al., 2003). Loosely apposed ectodermal cells condense into a sheet at the onset of zebrafish gastrulation (Concha and Adams, 1998). During internalization, lateral mesoderm disperses into single cells (Warga and Kimmel, 1990), which gradually reaggregate as they converge dorsally (Warga and Kimmel, 1990; Jessen et al., 2002), whereas dorsal mesoderm remains cohesive through dynamic cell-cell adhesion (Montero et al., 2005). Both germ layers show regulated adhesion; they dynamically modulate E-cadherin expression and acquire gap and tight junctions (Essner et al., 1996; Montero et al., 2005; Speirs et al., 2010). A secreted extracellular coat of fibronectin and laminin accumulates at the putative basal sides of the ectoderm and mesoderm, starting as discontinuous patches during gastrulation and becoming continuous by the end of gastrulation (Davidson et al., 2004; Latimer and Jessen, 2009). During segmentation stages, apical-basal polarity becomes overt by asymmetric distribution of classical markers. Asymmetric centrosome and cilia position in the somitic mesoderm has been observed as early as 14 hpf (10 somite stage) (Barrios et al., 2003; Borovina et al., 2010). Pard3 becomes apically localized by early segmentation stages (six or seven somites, 12 hpf) in cells of the neural tube (Tawk et al., 2007; Hong et al., 2010), accompanied by the tight junction marker ZO-1 (five- and 10-somite stage, 11.4 and 14 hpf) (Hong and Brewster, 2006; Yang et al., 2009) and polarity component aPKC (12 somites, 15 hpf) (Hong and Brewster, 2006). Furthermore, orientation of the MT cytoskeleton after 12 hpf (Hong et al., 2010) reveals the maturing apicobasal polarity in the neural epithelium. We suggest MTOC positioning is the earliest indicator of the nascent apical-basal polarity in ectoderm and mesoderm, and trace its origin to before mid-gastrulation.

Table 3. Anterior/posterior alignment of cell divisions

	Aligned	Not aligned	% Aligned	Number of cells	Number of embryos	Cells/embryo
Wild type (80%E)	19	7	73	26	11	2.4
Wild type (late gastrulae)	133	36	79	169	17	9.9
Ectoderm	101	22	82	123		
Mesoderm	32	14	69	46		
kny$^{fr6-/-}$	78	43	64	121	8	15.1
Xdd1	27	19	59	46	5	9.2

If the long axis of the dividing cell was within 45° of the anterior-posterior axis, it was counted as aligned.

The second type of polarity, a developing planar cell polarity, was exhibited by biased MTOC positions relative to the body axes in cells undergoing C&E movements. The centrosome organizes the MT cytoskeleton during gastrulation (Hong et al., 2010) (D.S.S. and L.S.-K., unpublished), as well as the Golgi complex, the proteasome and the cilium (Badano et al., 2005). Asymmetry in intracellular MTOC position indicates the location of these organelles and suggests possible planar polarity in their positions. During midgastrulation (8 hpf), the C&E movements of lateral mesodermal cells are thought to be Wnt/PCP independent (Jessen et al., 2002; Sepich and Solnica-Krezel, 2005). At this time, MTOCs exhibited a random or uniform distribution relative to the body axes (Fig. 3). By late gastrulation (after 9 hpf), dorsal ectoderm and mesoderm cells engage in fast C&E movements and display polarized phenotypes mediated by the Wnt/PCP pathway (Sepich et al., 2000; Jessen et al., 2002; Myers et al., 2002; Roszko et al., 2009). Our observations revealed MTOCs were non-randomly oriented relative to the body axes in these cells (Fig. 3), becoming biased towards the posterior and dorsal sides of cells. During the next hour, the positions of MTOC became biased either posterior-medial or posterior-lateral of the nucleus (Fig. 3). At this time, polarized radial intercalations and mediolateral intercalations are observed in the paraxial mesoderm (Yin et al., 2008). In cultured cells, MTOC and/or Golgi position are influenced by physical constraints of the cellular environment, cellular polarity and adhesive contacts. Many, but not all, cultured cell types migrate with a forward-biased MTOC (Yvon et al., 2002). However, the direction of migration of converging gastrula cells is not a good match for MTOC position until late gastrulation, when both MTOC and cell movements align in a dorsal direction. We hypothesize that changes in MTOC orientation may reflect changes in these polarized cell movements. Specifically, medial or lateral positioned MTOC may reflect medial or lateral cell intercalation, respectively. Ongoing time-lapse analyses will directly address this hypothesis. Earlier on, the average MTOC position is about 90° away from the movement direction. Thus, migration direction may have only a partial influence on MTOC positioning in cells engaged in C&E.

Spatial constraints play a role in MTOC position in cultured cells migrating over slender lines of fibronectin (Pouthas et al., 2008). These cells take a dramatically elongated shape with the MTOC trailing behind the nucleus. The MTOC/Golgi also takes a position that is rearward in the leading cells of the lateral line primordium in zebrafish embryos (Pouthas et al., 2008). Cells in the late gastrula elongate less than spindle-shaped cultured cells, but even this elongation might constrain MTOC position. Adhesion between a cell and its neighbors mediated by E- or N-cadherin (Desai et al., 2009; Dupin et al., 2009) or adhesion to substratum, i.e. fibronectin-coated micropatterns of different shapes, has also been shown to control MTOC and nuclear positions (Etienne-Manneville and Hall, 2001; Bornens, 2008). The cell-cell and cell-matrix adhesion could be involved in MTOC position during gastrulation, and testing this is an important future direction for research.

The timing of biased MTOC orientation indicated Wnt/PCP signaling could be a regulator of MTOC position. Wnt signaling, acting through Wnt5a and Dvl, works in parallel to Cdc42 to reorient MTOC in cultured cells (Schlessinger et al., 2007). Additionally, the co-receptor Ror2, and downstream effectors JNK and aPKCζ are involved (Nomachi et al., 2008). Our data are consistent with a role for Wnt/PCP signaling in influencing MTOC position during gastrulation. When Wnt/PCP signaling was disrupted in zebrafish gastrulae, MTOC position relative to the body axes was randomized, or assumed a weak anterior bias. We conclude that two components of Wnt/PCP signaling are required for cellular asymmetry visible in the orientation of the MTOC. Surprisingly, our preliminary studies suggest normal MTOC distributions in *trilobite/vangl2* zygotic mutants, implying Vangl2 is not essential for this aspect of MT polarity (D.S.S., Roszko, I. and L.S.-K., unpublished). Finally, whether Wnt/PCP signaling can effect the distribution of growing tips of MTs has not been tested in this system. Another report (Shindo et al., 2008) shows that distribution of growing MT tips is unaffected by loss of Wnt/PCP signaling in *Xenopus* notochord.

MTs are required for the establishment, but not maintenance, of AP polarization of cells during gastrulation

Previous studies have suggested that C&E gastrulation movements are adversely affected by loss of intact MTs (Strahle and Jesuthasan, 1993; Solnica-Krezel and Driever, 1994). Similarly, in *Xenopus*, MTs are involved in initiation of gastrulation (Lane and Keller, 1997; Lee and Harland, 2007), and later MTs maintain an organized actin cytoskeleton to allow cell contacts and protrusions in the involuting mesoderm (Kwan and Kirschner, 2005). Our studies show reciprocal interactions between Wnt/PCP signaling and the MT cytoskeleton during gastrulation. As discussed above, Wnt/PCP biased intracellular position of MTOC. Conversely, our MT disruption experiments at mid- or late gastrulation revealed that MTs are needed for the initial clustering and localization of *Drosophila* Prickle-GFP at the anterior cell membrane (and, thus, for a step in AP polarization of cells engaged in C&E). Disruption of MTs by nocodazole treatment at late gastrulation caused only a few cells to round and lose anterior Pk spots; most cells remained elongated with anteriorly accumulated Pk-GFP. Therefore, MTs are needed for the establishment, but not for maintenance, of the anterior Pk-GFP localization and mediolateral cell elongation. Kwan and Kirschner (Kwan and Kirschner, 2005) observed two distinct time-dependent responses of actin to MT depolymerization. Brief exposure to nocodazole strongly reduced the number and extent of lamellipodial protrusions. Long exposure caused cell rounding and loss of cell-cell contacts. Therefore, MTs may be needed to maintain cell contacts, which in turn may be required for anterior identity to be established. Alternatively, the loss of Pk puncta resulting from early treatment with nocodazole may show a direct role for the MT cytoskeleton in the transport or clustering of Pk at the anterior membrane, as in asymmetric transport of Fz observed in *Drosophila* wing epithelia (Shimada et al., 2006).

The mesoderm has intrinsic AP pattern that is interpreted by Wnt/PCP signaling to guide C&E (Ninomiya et al., 2004). For example, alignment of cell division (Concha and Adams, 1998; Gong et al., 2004) (Table 3) and polarized directed migration are oriented relative to the AP axis and require intact PCP signaling. Polarized planar and radial intercalations contribute to axis elongation by preferentially separating anterior and posterior neighbors in a Wnt/PCP-dependent manner (Yin et al., 2008). AP patterning is also revealed by asymmetric localization of Wnt/PCP proteins and cellular organelles, with Pk-GFP localizing to the anterior (Ciruna et al., 2006) and Dvl-GFP to the posterior edges of cells engaged in C&E (Yin et al., 2009). Recently, studies in zebrafish and mouse showed that centrosomes and cilia in the floor plate of the neural tube, and in the asymmetry organs (Kupffer's vesicle and node) during segmentation stages, are found at the posterior side of the cell in a Wnt/PCP-dependent fashion (Borovina et al., 2010; Hashimoto et al., 2010).

Our studies also reveal posterior bias of MTOC localization that is first detected at late gastrulation, coincident with AP polarization of cells engaged in C&E (Topczewski et al., 2001; Yin et al., 2008). It is tempting to speculate that the posterior bias of MTOC we observe during gastrulation is a precursor of posterior localization of cilia found at later stages of development. Hence, the AP cell polarization established by Wnt/PCP signaling during gastrulation is maintained by tissues at later stages of embryogenesis. We propose a model of reciprocal Wnt/PCP and MT interactions in which Wnt /PCP signaling shapes the MT cytoskeleton by biasing the intracellular position of the centrosome and possibly dependent organelles. In turn, Wnt/PCP signaling requires MT function so it can respond to global AP positional information by enriching Wnt/PCP components at anterior or posterior cell edges and mediate polarized cell movement behaviors underlying C&E.

Acknowledgements
We thank Christina Speirs, Dan Carlin and Isabelle Roszko for comments, and the following researchers for providing reagents: Masa Tada for Dvl clones, Kristin Kwan and Adrian Salic for the eGFP-Xcentrin clone; and Brian Ciruna and Andreas Jenny for the Drosophila Pk-GFP clone. Experiments were performed in facilities funded by Vanderbilt University Academic Venture Capital Fund and VUMC Cell Imaging Core Facility (NIH grant 1S10RR015682). This work was supported by NIH R01 (GM55101) and a grant from Human Frontiers in Science Program. Deposited in PMC for release after 12 months.

Competing interests statement
The authors declare no competing financial interests.

Supplementary material
Supplementary material for this article is available at
http://dev.biologists.org/lookup/suppl/doi:10.1242/dev.053959/-/DC1

References
Adler, P. N. (2002). Planar signaling and morphogenesis in Drosophila. *Dev. Cell* **2**, 525-535.
Amonlirdviman, K., Khare, N. A., Tree, D. R., Chen, W. S., Axelrod, J. D. and Tomlin, C. J. (2005). Mathematical modeling of planar cell polarity to understand domineering nonautonomy. *Science* **307**, 423-426.
Axelrod, J. D. (2001). Unipolar membrane association of Dishevelled mediates Frizzled planar cell polarity signaling. *Genes Dev.* **15**, 1182-1187.
Axelrod, J. D. (2009). Progress and challenges in understanding planar cell polarity signaling. *Semin. Cell Dev. Biol.* **20**, 964-971.
Axelrod, J. D. and McNeill, H. (2002). Coupling planar cell polarity signaling to morphogenesis. *Scientific World Journal* **2**, 434-454.
Badano, J. L., Teslovich, T. M. and Katsanis, N. (2005). The centrosome in human genetic disease. *Nat. Rev. Genet.* **6**, 194-205.
Barrios, A., Poole, R. J., Durbin, L., Brennan, C., Holder, N. and Wilson, S. W. (2003). Eph/Ephrin signaling regulates the mesenchymal-to-epithelial transition of the paraxial mesoderm during somite morphogenesis. *Curr. Biol.* **13**, 1571-1582.
Bastock, R., Strutt, H. and Strutt, D. (2003). Strabismus is asymmetrically localised and binds to Prickle and Dishevelled during Drosophila planar polarity patterning. *Development* **130**, 3007-3014.
Baum, B., Settleman, J. and Quinlan, M. P. (2008). Transitions between epithelial and mesenchymal states in development and disease. *Semin. Cell Dev. Biol.* **19**, 294-308.
Bornens, M. (2008). Organelle positioning and cell polarity. *Nat. Rev. Mol. Cell Biol.* **9**, 874-886.
Borovina, A., Superina, S., Voskas, D. and Ciruna, B. (2010). Vangl2 directs the posterior tilting and asymmetric localization of motile primary cilia. *Nat. Cell Biol.* **12**, 407-412.
Cha, S. W., Tadjuidje, E., Tao, Q., Wylie, C. and Heasman, J. (2008). Wnt5a and Wnt11 interact in a maternal Dkk1-regulated fashion to activate both canonical and non-canonical signaling in Xenopus axis formation. *Development* **135**, 3719-3729.
Ciruna, B., Jenny, A., Lee, D., Mlodzik, M. and Schier, A. F. (2006). Planar cell polarity signalling couples cell division and morphogenesis during neurulation. *Nature* **439**, 220-224.
Concha, M. L. and Adams, R. J. (1998). Oriented cell divisions and cellular morphogenesis in the zebrafish gastrula and neurula: a time-lapse analysis. *Development* **125**, 983-994.
Davidson, L. A., Keller, R. and DeSimone, D. W. (2004). Assembly and remodeling of the fibrillar fibronectin extracellular matrix during gastrulation and neurulation in Xenopus laevis. *Dev. Dyn.* **231**, 888-895.
Dawe, H. R., Smith, U. M., Cullinane, A. R., Gerrelli, D., Cox, P., Badano, J. L., Blair-Reid, S., Sriram, N., Katsanis, N., Attie-Bitach, T. et al. (2007). The Meckel-Gruber Syndrome proteins MKS1 and meckelin interact and are required for primary cilium formation. *Hum. Mol. Genet.* **16**, 173-186.
Desai, R. A., Gao, L., Raghavan, S., Liu, W. F. and Chen, C. S. (2009). Cell polarity triggered by cell-cell adhesion via E-cadherin. *J. Cell Sci.* **122**, 905-911.
Dupin, I., Camand, E. and Etienne-Manneville, S. (2009). Classical cadherins control nucleus and centrosome position and cell polarity. *J. Cell Biol.* **185**, 779-786.
Eaton, S. (2003). Cell biology of planar polarity transmission in the Drosophila wing. *Mech. Dev.* **120**, 1257-1264.
Essner, J. J., Laing, J. G., Beyer, E. C., Johnson, R. G. and Hackett, P. B., Jr (1996). Expression of zebrafish connexin43.4 in the notochord and tail bud of wild-type and mutant no tail embryos. *Dev. Biol.* **177**, 449-462.
Etienne-Manneville, S. and Hall, A. (2001). Integrin-mediated activation of Cdc42 controls cell polarity in migrating astrocytes through PKCzeta. *Cell* **106**, 489-498.
Fanto, M. and McNeill, H. (2004). Planar polarity from flies to vertebrates. *J. Cell Sci.* **117**, 527-533.
Feiguin, F., Hannus, M., Mlodzik, M. and Eaton, S. (2001). The ankyrin repeat protein Diego mediates Frizzled-dependent planar polarization. *Dev. Cell* **1**, 93-101.
Gong, Y., Mo, C. and Fraser, S. E. (2004). Planar cell polarity signalling controls cell division orientation during zebrafish gastrulation. *Nature* **430**, 689-693.
Goto, T., Davidson, L., Asashima, M. and Keller, R. (2005). Planar cell polarity genes regulate polarized extracellular matrix deposition during frog gastrulation. *Curr. Biol.* **15**, 787-793.
Gubb, D. and Garcia-Bellido, A. (1982). A genetic analysis of the determination of cuticular polarity during development in Drosophila melanogaster. *J. Embryol. Exp. Morphol.* **68**, 37-57.
Hashimoto, M., Shinohara, K., Wang, J., Ikeuchi, S., Yoshiba, S., Meno, C., Nonaka, S., Takada, S., Hatta, K., Wynshaw-Boris, A. et al. (2010). Planar polarization of node cells determines the rotational axis of node cilia. *Nat. Cell Biol.* **12**, 170-176.
Hay, E. D. (2005). The mesenchymal cell, its role in the embryo, and the remarkable signaling mechanisms that create it. *Dev. Dyn.* **233**, 706-720.
Hong, E. and Brewster, R. (2006). N-cadherin is required for the polarized cell behaviors that drive neurulation in the zebrafish. *Development* **133**, 3895-3905.
Hong, E., Jayachandran, P. and Brewster, R. (2010). The polarity protein Pard3 is required for centrosome positioning during neurulation. *Dev. Biol.* **341**, 335-345.
Jenny, A., Darken, R. S., Wilson, P. A. and Mlodzik, M. (2003). Prickle and Strabismus form a functional complex to generate a correct axis during planar cell polarity signaling. *EMBO J.* **22**, 4409-4420.
Jessen, J. R., Topczewski, J., Bingham, S., Sepich, D. S., Marlow, F., Chandrasekhar, A. and Solnica-Krezel, L. (2002). Zebrafish trilobite identifies new roles for Strabismus in gastrulation and neuronal movements. *Nat. Cell Biol.* **4**, 610-615.
Jiang, D., Munro, E. M. and Smith, W. C. (2005). Ascidian prickle regulates both mediolateral and anterior-posterior cell polarity of notochord cells. *Curr. Biol.* **15**, 79-85.
Jones, C. and Chen, P. (2008). Primary cilia in planar cell polarity regulation of the inner ear. *Curr. Top. Dev. Biol.* **85**, 197-224.
Keller, R. (2002). Shaping the vertebrate body plan by polarized embryonic cell movements. *Science* **298**, 1950-1954.
Kimmel, C. B., Ballard, W. W., Kimmel, S. R., Ullmann, B. and Schilling, T. F. (1995). Stages of embryonic development of the zebrafish. *Dev. Dyn.* **203**, 253-310.
Kwan, K. M. and Kirschner, M. W. (2005). A microtubule-binding Rho-GEF controls cell morphology during convergent extension of Xenopus laevis. *Development* **132**, 4599-4610.
Lane, M. C. and Keller, R. (1997). Microtubule disruption reveals that Spemann's organizer is subdivided into two domains by the vegetal alignment zone. *Development* **124**, 895-906.
Latimer, A. and Jessen, J. R. (2009). Extracellular matrix assembly and organization during zebrafish gastrulation. *Matrix Biol.* **29**, 89-96.
Lee, J. Y. and Harland, R. M. (2007). Actomyosin contractility and microtubules drive apical constriction in Xenopus bottle cells. *Dev. Biol.* **311**, 40-52.
Marlow, F., Topczewski, J., Sepich, D. and Solnica-Krezel, L. (2002). Zebrafish Rho kinase 2 acts downstream of Wnt11 to mediate cell polarity and effective convergence and extension movements. *Curr. Biol.* **12**, 876-884.
Mikels, A. J. and Nusse, R. (2006). Purified Wnt5a protein activates or inhibits beta-catenin-TCF signaling depending on receptor context. *PLoS Biol.* **4**, e115.
Mikels, A., Minami, Y. and Nusse, R. (2009). Ror2 receptor requires tyrosine kinase activity to mediate Wnt5A signaling. *J Biol. Chem.* **284**, 30167-30176.

Montero, J. A., Carvalho, L., Wilsch-Brauninger, M., Kilian, B., Mustafa, C. and Heisenberg, C. P. (2005). Shield formation at the onset of zebrafish gastrulation. *Development* **132**, 1187-1198.
Mullins, M. C., Hammerschmidt, M., Kane, D. A., Odenthal, J., Brand, M., van Eeden, F. J., Furutani-Seiki, M., Granato, M., Haffter, P., Heisenberg, C. P. et al. (1996). Genes establishing dorsoventral pattern formation in the zebrafish embryo: the ventral specifying genes. *Development* **123**, 81-93.
Myers, D. C., Sepich, D. S. and Solnica-Krezel, L. (2002). Bmp activity gradient regulates convergent extension during zebrafish gastrulation. *Dev. Biol.* **243**, 81-98.
Narayan, S., Jaiswal, A. S., Kang, D., Srivastava, P., Das, G. M. and Gairola, C. G. (2004). Cigarette smoke condensate-induced transformation of normal human breast epithelial cells in vitro. *Oncogene* **23**, 5880-5889.
Ninomiya, H., Elinson, R. P. and Winklbauer, R. (2004). Antero-posterior tissue polarity links mesoderm convergent extension to axial patterning. *Nature* **430**, 364-367.
Nomachi, A., Nishita, M., Inaba, D., Enomoto, M., Hamasaki, M. and Minami, Y. (2008). Receptor tyrosine kinase Ror2 mediates Wnt5a-induced polarized cell migration by activating c-Jun N-terminal kinase via actin-binding protein filamin A. *J. Biol. Chem.* **283**, 27973-27981.
Park, T. J., Mitchell, B. J., Abitua, P. B., Kintner, C. and Wallingford, J. B. (2008). Dishevelled controls apical docking and planar polarization of basal bodies in ciliated epithelial cells. *Nat. Genet.* **40**, 871-879.
Piel, M., Meyer, P., Khodjakov, A., Rieder, C. L. and Bornens, M. (2000). The respective contributions of the mother and daughter centrioles to centrosome activity and behavior in vertebrate cells. *J. Cell Biol.* **149**, 317-330.
Pouthas, F., Girard, P., Lecaudey, V., Ly, T. B., Gilmour, D., Boulin, C., Pepperkok, R. and Reynaud, E. G. (2008). In migrating cells, the Golgi complex and the position of the centrosome depend on geometrical constraints of the substratum. *J. Cell Sci.* **121**, 2406-2414.
Roszko, I., Sawada, A. and Solnica-Krezel, L. (2009). Regulation of convergence and extension movements during vertebrate gastrulation by the Wnt/PCP pathway. *Semin. Cell Dev. Biol.* **20**, 986-997.
Saude, L., Woolley, K., Martin, P., Driever, W. and Stemple, D. L. (2000). Axis-inducing activities and cell fates of the zebrafish organizer. *Development* **127**, 3407-3417.
Schlessinger, K., McManus, E. J. and Hall, A. (2007). Cdc42 and noncanonical Wnt signal transduction pathways cooperate to promote cell polarity. *J. Cell Biol.* **178**, 355-361.
Sepich, D. S. and Solnica-Krezel, L. (2005). Analysis of cell movements in zebrafish embryos: morphometrics and measuring movement of labeled cell populations in vivo. *Methods Mol. Biol.* **294**, 211-233.
Sepich, D. S., Myers, D. C., Short, R., Topczewski, J., Marlow, F. and Solnica-Krezel, L. (2000). Role of the zebrafish trilobite locus in gastrulation movements of convergence and extension. *Genesis* **27**, 159-173.
Sepich D. S., Calmelet C., Kiskowski M. and Solnica-Krezel L. (2005). Initiation of convergence and extension movements of lateral mesoderm during zebrafish gastrulation. *Dev. Dyn.* **234**, 279-292.
Shimada, Y., Usui, T., Yanagawa, S., Takeichi, M. and Uemura, T. (2001). Asymmetric colocalization of Flamingo, a seven-pass transmembrane cadherin, and Dishevelled in planar cell polarization. *Curr. Biol.* **11**, 859-863.
Shimada, Y., Yonemura, S., Ohkura, H., Strutt, D. and Uemura, T. (2006). Polarized transport of Frizzled along the planar microtubule arrays in Drosophila wing epithelium. *Dev. Cell* **10**, 209-222.
Shindo, A., Yamamoto, T. S. and Ueno, N. (2008). Coordination of cell polarity during Xenopus gastrulation. *PLoS ONE* **3**, e1600.
Simons, M. and Mlodzik, M. (2008). Planar cell polarity signaling: from fly development to human disease. *Annu. Rev. Genet.* **42**, 517-540.
Solnica-Krezel, L. (2005). Conserved patterns of cell movements during vertebrate gastrulation. *Curr. Biol.* **15**, R213-R228.
Solnica-Krezel, L. and Driever, W. (1994). Microtubule arrays of the zebrafish yolk cell: organization and function during epiboly. *Development* **120**, 2443-2455.
Solnica-Krezel, L., Schier, A. F. and Driever, W. (1994). Efficient recovery of ENU-induced mutations from the zebrafish germline. *Genetics* **136**, 1401-1420.
Speirs, C. K., Jernigan, K. K., Kim, S. H., Cha, Y. I., Lin, F., Sepich, D. S., DuBois, R. N., Lee, E. and Solnica-Krezel, L. (2010). Prostaglandin Gbetagamma signaling stimulates gastrulation movements by limiting cell adhesion through Snai1a stabilization. *Development* **137**, 1327-1337.
Strahle, U. and Jesuthasan, S. (1993). Ultraviolet irradiation impairs epiboly in zebrafish embryos: evidence for a microtubule-dependent mechanism of epiboly. *Development* **119**, 909-919.
Strutt, D. I. (2001). Asymmetric localization of frizzled and the establishment of cell polarity in the Drosophila wing. *Mol. Cell* **7**, 367-375.
Strutt, D. and Strutt, H. (2007). Differential activities of the core planar polarity proteins during Drosophila wing patterning. *Dev. Biol.* **302**, 181-194.
Strutt, H. and Strutt, D. (2009). Asymmetric localisation of planar polarity proteins: mechanisms and consequences. *Semin. Cell Dev. Biol.* **20**, 957-963.
Tada, M. and Smith, J. C. (2000). Xwnt11 is a target of Xenopus Brachyury: regulation of gastrulation movements via Dishevelled, but not through the canonical Wnt pathway. *Development* **127**, 2227-2238.
Tawk, M., Araya, C., Lyons, D. A., Reugels, A. M., Girdler, G. C., Bayley, P. R., Hyde, D. R., Tada, M. and Clarke, J. D. (2007). A mirror-symmetric cell division that orchestrates neuroepithelial morphogenesis. *Nature* **446**, 797-800.
Thiery, J. P. (2002). Epithelial-mesenchymal transitions in tumour progression. *Nat. Rev. Cancer* **2**, 442-454.
Topczewski, J., Sepich, D. S., Myers, D. C., Walker, C., Amores, A., Lele, Z., Hammerschmidt, M., Postlethwait, J. and Solnica-Krezel, L. (2001). The zebrafish glypican knypek controls cell polarity during gastrulation movements of convergent extension. *Dev. Cell* **1**, 251-264.
Tree, D. R., Shulman, J. M., Rousset, R., Scott, M. P., Gubb, D. and Axelrod, J. D. (2002). Prickle mediates feedback amplification to generate asymmetric planar cell polarity signaling. *Cell* **109**, 371-381.
Ulrich, F., Krieg, M., Schotz, E. M., Link, V., Castanon, I., Schnabel, V., Taubenberger, A., Mueller, D., Puech, P. H. and Heisenberg, C. P. (2005). Wnt11 functions in gastrulation by controlling cell cohesion through Rab5c and E-cadherin. *Dev. Cell* **9**, 555-564.
Usui, T., Shima, Y., Shimada, Y., Hirano, S., Burgess, R. W., Schwarz, T. L., Takeichi, M. and Uemura, T. (1999). Flamingo, a seven-pass transmembrane cadherin, regulates planar cell polarity under the control of Frizzled. *Cell* **98**, 585-595.
Wallingford, J. B., Rowning, B. A., Vogeli, K. M., Rothbacher, U., Fraser, S. E. and Harland, R. M. (2000). Dishevelled controls cell polarity during Xenopus gastrulation. *Nature* **405**, 81-85.
Warga, R. M. and Kimmel, C. B. (1990). Cell movements during epiboly and gastrulation in zebrafish. *Development* **108**, 569-580.
Wu, J. and Mlodzik, M. (2008). The frizzled extracellular domain is a ligand for Van Gogh/Stbm during nonautonomous planar cell polarity signaling. *Dev. Cell* **15**, 462-469.
Yang, X., Zou, J., Hyde, D. R., Davidson, L. A. and Wei, X. (2009). Stepwise maturation of apicobasal polarity of the neuroepithelium is essential for vertebrate neurulation. *J. Neurosci.* **29**, 11426-11440.
Yin, C. and Solnica-Krezel, L. (2007). Convergence and extension movements mediate the specification and fate maintenance of zebrafish slow muscle precursors. *Dev. Biol.* **304**, 141-155.
Yin, C., Kiskowski, M., Pouille, P. A., Farge, E. and Solnica-Krezel, L. (2008). Cooperation of polarized cell intercalations drives convergence and extension of presomitic mesoderm during zebrafish gastrulation. *J. Cell Biol.* **180**, 221-232.
Yvon, A. M., Walker, J. W., Danowski, B., Fagerstrom, C., Khodjakov, A. and Wadsworth, P. (2002). Centrosome reorientation in wound-edge cells is cell type specific. *Mol. Biol. Cell* **13**, 1871-1880.